*marine drugs*

MDPI

*Article*

# Content, Ratio and Productivity of Amphidinols in Wild-Type and Mutagenized Strains of *Amphidinium carterae* at Different Growth Stages

**Ivan Citakovic [1,2,*], Gaël Bougaran [2], Fabienne Hervé [2], Damien Réveillon [2], Cyril El Khoury [1], Francis Mairet [2] and Bruno Saint-Jean [2]**

[1] Immunrise Biocontrol France (IBF), 2 Chemine des Arestieux, 33610 Cestas, France
[2] Ifremer, PHYTOX, 44000 Nantes, France
* Correspondence: ivan@immunrisebiocontrol.fr or contact@immunrisebiocontrol.fr

**Abstract**

As agriculture faces increasing pressure to reduce pesticide residues and heavy metal accumulation in soils, marine microalgae are emerging as sustainable sources of biopesticides. Among them, *Amphidinium carterae* produces amphidinols (AMs), polyketide metabolites with strong antifungal activity against crop pathogens. Currently, large-scale AM production remains constrained by a limited understanding of AM biosynthesis across different *A. carterae* growth phases and by the lack of high-performing industrial strains. In this study, AM production dynamics were investigated in one wild-type (WT) and five mutagenized *A. carterae* strains. The production of bioactive AM18 and its sulfated inactive form AM19 was monitored through exponential, linear, and early stationary growth phases. The maximum AM productivity occurred between the linear and early stationary phase, with the average values of 5.58 ± 0.4 and 3.58 ± 0.2 µg/mL/day for AM18 and AM19, respectively. The AM18/AM19 ratio consistently decreased with the culture age, indicating that earlier harvesting favors higher proportions of bioactive AMs. UV mutagenesis increased the AM18 cell content by more than twofold and the growth rate by up to 20% in certain mutagenized strains compared to the WT strain, but did not enhance the volumetric AM productivity. Overall, these results identify optimal AM harvesting windows and clarify the potential benefits of mutagenesis strain improvement for industrial AM production improvement.

**Keywords:** amphidinols; cell content; productivity; growth phase; batch cultivation; photobioreactor

Check for updates

Academic Editor: Maria Elena Barone

Received: 30 December 2025
Revised: 6 February 2026
Accepted: 10 February 2026
Published: 12 February 2026

**Copyright:** © 2026 by the authors. Licensee MDPI, Basel, Switzerland. This article is an open access article distributed under the terms and conditions of the Creative Commons Attribution (CC BY) license.

## 1. Introduction

In the modern world, soil contamination is an increasing concern even in the regions committed to ecological transition such as the EU. Agriculture is identified as one of the major contributors, particularly through the release of pesticide residues and heavy metals. In a study led by the EU Soil Observatory, pesticidal residues were detected in 74.5% of assessed agricultural soils, with mixtures of multiple residues found in 57.1% of these sites [1]. Over the decades, the widespread use of pesticides based on heavy metals like copper has led to increasing doses of these metals in the soil [2]. Interestingly, copper-based biopesticides are compliant with organic-certified agricultural practices [3]. Such legislation has left even organically cultivated lands at risk of heavy metal pollution. Therefore, rethinking existing agricultural practices may be an important step in reducing soil contamination and pollutant accumulation in the food chain.

As a nature-based solution for crop protection, biopesticides have piqued a significant amount of interest in the last decade. From 2018 to 2022, the biopesticide sector expanded at a compound annual growth rate (CAGR) of 11.0%, while reaching the value of US $ 8123 million in 2023 [4]. Looking ahead, the trend is expected to continue, with forecasts showing a 10.3% CAGR that will bring the biopesticide market to an estimated US $ 21.8 billion by 2033 [4]. The regulatory framework in regions like the EU also facilitated the increased use of biopesticides. For example, the EU Commission's Green Deal proposed reducing the use of chemical pesticides by 50% by 2030 [5], thereby promoting biopesticides as alternatives to conventional pesticides. However, meeting the growing demand for biopesticides may require digging deeper into the biological diversity of unexplored habitats and discovering new bioactive metabolites that could serve as biopesticide candidates.

Microalgae and cyanobacteria are increasingly recognized as a promising natural source for future biopesticide compounds, as underlined in various scientific reviews [6,7]. In particular, several microalgal and cyanobacterial secondary metabolites have demonstrated remarkable biocidal activity, attracting attention for their potential use as biopesticides, including laxaphycins from *Anabaena laxa* [8], anatoxin-A and related anatoxins from the same genus [9], microcystins from *Microcystis aeruginosa* [10], and amphidinols from *Amphidinium carterae* [11]. Nevertheless, despite the growing scientific evidence supporting their potential, microalgae- and cyanobacteria-based biopesticides have not yet entered the market. This outcome is largely explained by difficulties in scaling up cultivation, the long and expensive authorization procedures for new biopesticides, and the absence of high-performance industrial strains producing targeted biopesticides [12].

*Amphidinium* is a genus of dinoflagellate microalgae comprising approximately 20 species [13], which belong to the family *Amphidiniaceae* [14,15]. The members of the genus *Amphidinium* are cosmopolitan and have been reported in aquatic environments ranging from temperate [16] to tropical waters [17], with *A. carterae, A. klebsii*, and *A. operculatum* being among the most widely reported and studied species [18]. Species of the genus *Amphidinium* are known to produce a wide range of bioactive molecules including amdigenols, amphidinolides, amphidinols, iriomoteolides and amphidolactones [19]. Among these, amphidinols (AMs) are one of the most studied families, comprising more than 30 analogs [20], with new family members being described almost yearly. Amphidinols are characterized by a core structure containing two tetrahydropyran rings connected through a six-carbon linker. This core is accompanied by a polyunsaturated, lipophilic alkyl chain and a hydrophilic arm rich in hydroxyl groups with more than 15 carbons in the chain [21]. Even though the exact natural role of the AMs is not known, some studies suggest their role in defending against predators and competing with other microalgal species, as is the case for structurally similar karlotoxins [22]. Numerous AMs produced by *Amphidinium carterae* have exhibited antimicrobial activity against a wide range of fungi and bacteria. The mode of action of AMs against microbes lies in their ability to disrupt plasma membrane integrity through their incorporation into the cell membrane and pore formation [23]. The remarkable antifungal activity of AMs was observed against *Aspergillus niger*, *Aspergillus fumigatus* and *Candida albicans*. For instance, AM22 was shown to inhibit *A. fumigatus* with a MIC of 64 µg/mL [24], while AM18 demonstrated to be highly active against *C. albicans*, with a MIC of 9 µg/mL [21]. In addition to their antifungal effects, several amphidinols have also exhibited antibacterial properties, with AM-A exhibiting MICs of 16 µg/mL against *Staphylococcus aureus* and 64 µg/mL against *Enterococcus faecium* [25]. Altogether, these and other results in the literature highlight the broad antimicrobial potential of this family of molecules.

However, it is important to note that not all amphidinols are potent antimicrobial compounds. Notably, the presence of certain chemical groups, like sulfates, can greatly diminish the antimicrobial potency of AMs, as highlighted in various studies [21,26]. For example, Nuzzo and colleagues reported that AM18 exhibited an MIC of 9 µg/mL against *Candida albicans*, whereas its sulfated form, AM19, showed no antifungal effect against this microorganism [21]. Similarly, the sulfation of other AMs has been found to considerably lower or fully eliminate their antimicrobial activity when compared to their non-sulfated forms [27].

Growing evidence of the antimicrobial potential of certain AM family members has attracted interest in their use against fungal pathogens in agriculture. Moreover, the first patents have been established on the use of AMs as biopesticides [11]. Nevertheless, to scale up the economically feasible production of AMs from *A. carterae*, there is a noticeable need to (i) optimize algal cultivation strategies (batch, fed batch, or continuous) along with associated culture conditions, and (ii) perform efficient strain improvement. With regard to the first point, previous studies have shown that amphidinol production in *A. carterae* is influenced by culture conditions such as nutrient availability, light regime, and cultivation duration, which affect both cellular content and volumetric productivity [28–30]. These findings highlight the importance of optimizing mentioned culture parameters to achieve optimal AM production.

However, a major obstacle to the rational optimization of *A. carterae* cultivation modes remains the limited understanding of AM production kinetics across distinct microalgal growth phases. This knowledge may be crucial in defining the right time point for AM harvesting suitable for each of the culturing modes that may be used for *A. carterae* production (e.g., semi-batch or continuous).

In our previous study, the dynamics of AMs during the stationary phase of *A. carterae* were investigated [29]. However, to the best of our knowledge, no other study has described the evolution of AM concentrations in culture growth phases before reaching the growth plateau. In this study, amphidinol concentration dynamics were compared across three growth phases (exponential, linear, and early stationary) in one WT and five mutagenized *A. carterae* strains. Moreover, because the *A. carterae* strains produce both active and inactive amphidinols (AM18 and AM19), the evolution of the AM18/AM19 ratio was monitored across growth phases to identify the optimal harvesting stage for the highest proportion of bioactive AMs. Finally, this study compared the AM production dynamics between one WT and five mutagenized *A. carterae* strains, thereby assessing the potential of random mutagenesis to enhance AM production in *A. carterae*.

## 2. Results and Discussion

### *2.1. Growth Dynamics of WT and Mutagenized A. carterae Strains*

Figure 1 presents the growth kinetics of the wild-type and the five mutagenized *A. carterae* strains grown under the same culture conditions, with one fitted growth curve shown for each strain.

Overall, the mutagenized strains exhibited similar or slightly elevated stationary phase cell concentrations compared to the WT strain (Table 1), as can be seen when comparing the A values among the strains, which reflect the asymptotic maximum biomass reached at the stationary phase of growth. Strain 1.6 B6 reached the highest A value (2.503 ± 0.040), closely followed by 1.5 C4 (2.485 ± 0.044), whereas strain 1.8 B3 displayed the lowest value (2.318 ± 0.024), slightly below that of the WT (2.396 ± 0.039). Even though the one-way ANOVA, which used the WT strain as the reference, showed that the A values of all the mutagenized strains were statistically different from those of the WT with significance $p < 0.01$ (see Appendix A Table A1. for the comparison of the *p*-values of each WT and

mutagenized strain), the magnitude of these differences was too small to be considered biologically meaningful.

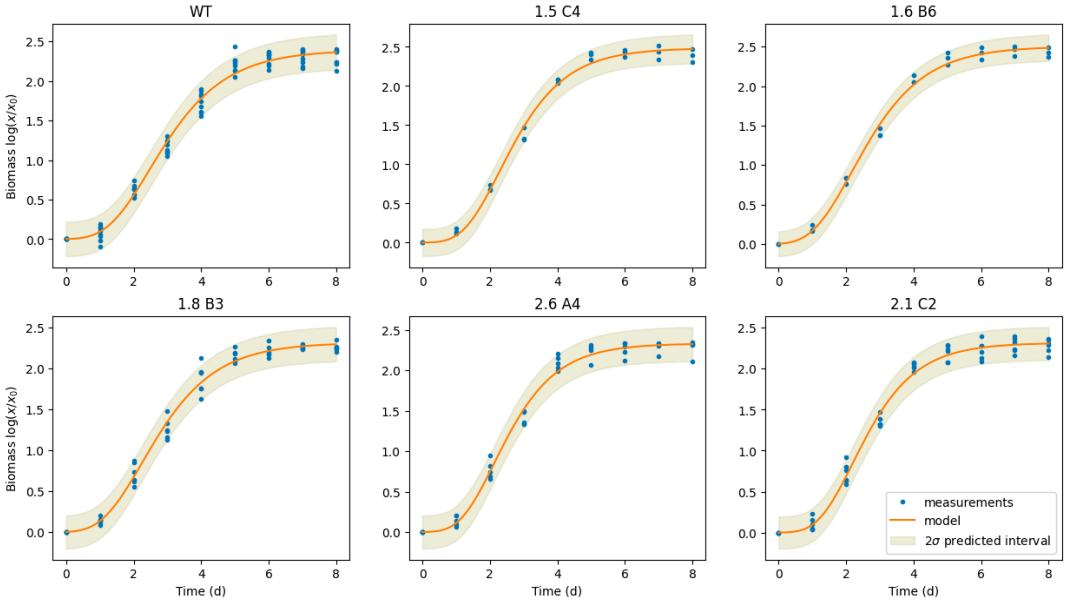


**Figure 1.** Growth dynamics of WT and the five mutagenized *A. carterae* strains. Blue dots on each figure represent the experimental measurements for all of the culture replicates for one strain, while the orange line indicates the fitted growth curve based on the modified Gompertz equation (see methodology; Section 3.2.2) used to model growth based on all these data points. The shaded area around the curve represents the two-standard-deviation (2 SD) prediction interval of the model.

**Table 1.** Culture parameters estimated from the modified logistic growth model for the wild-type and the five mutated strains of *Amphidinium carterae*. For each strain, the parameters A and $\mu_{max}$ were fitted independently for every replicate across all of the strains, and the table presents the mean and standard deviation of these values for each strain.

| Strain | A (±SD) | $\mu_{max}$ (Day$^{-1}$ ± SD) | Replicate Number |
|---|---|---|---|
| WT | 2.396 ± 0.039 | 0.705 ± 0.014 | 9 |
| 1.5 C4 | 2.485 ± 0.044 | 0.844 ± 0.009 | 3 |
| 1.6 B6 | 2.503 ± 0.040 | 0.774 ± 0.010 | 3 |
| 1.8 B3 | 2.318 ± 0.024 | 0.721 ± 0.035 | 6 |
| 2.6 A4 | 2.332 ± 0.041 | 0.843 ± 0.017 | 5 |
| 2.1 C2 | 2.315 ± 0.043 | 0.833 ± 0.020 | 6 |

The maximum specific growth rates ($\mu_{max}$) varied across strains, with the fastest rate observed in strain 1.5 C4 (0.844 ± 0.009 day$^{-1}$), closely followed by strains 2.6 A4 (0.843 ± 0.017 day$^{-1}$) and 2.1 C2 (0.833 ± 0.020 day$^{-1}$). The WT and 1.8 B3 strains showed the lowest $\mu_{max}$ values (0.705 ± 0.014 and 0.721 ± 0.035 day$^{-1}$, respectively). Notably, strain 1.5 C4 displayed an increase in $\mu_{max}$ greater than 20%, which makes it of potential industrial interest, provided that AM productivity is not negatively affected. The one-way ANOVA test, using WT as a reference, followed by the Holm–Sidak post hoc test, revealed that the $\mu_{max}$ values of all the mutagenized strains except 1.8 B3 were significantly higher than those of the WT (see Appendix A Table A1 for the *p*-values). These statistical results indicate that random mutagenesis can increase the maximal growth rate in *A. carterae*.

Finally, after 8 days of growth, an additional quantity of nitrate was added to one culture replicate of the WT, 1.8 B3, and 2.6 A4 strains (strains and replicates were chosen randomly) to assess whether the stationary phase observed under the tested conditions

was caused by nitrogen limitation (see Section 3.1.5). This assessment was important because it allowed for a more direct comparison of this research with previous studies on AM production in *A. carterae*, which were mainly performed under nitrogen-limited conditions [28,29].

Nitrogen supplementation was chosen as a technique to test nitrogen limitation instead of measuring extracellular nitrate concentrations, as depleted nitrogen levels in the growth medium do not necessarily indicate nitrogen limitation as is commonly believed. Indeed, microalgal cells can retain assimilated nitrogen in intracellular pools, which may sustain further growth even when external nitrogen appears to be depleted.

When the mentioned WT, 1.8 B3 and 2.6 A4 cultures entered the stationary phase, their cell concentrations reached $1.74 \times 10^6$, $1.68 \times 10^6$ and $1.69 \times 10^6$ cell/mL, respectively. After the addition of nitrogen, the cultures grew again and eventually reached a new stationary phase, with the respective cell concentrations of $2.31 \times 10^6$, $2.19 \times 10^6$ and $2.15 \times 10^6$ cell/mL. Such concentration elevations indicated that nitrogen was the growth-limiting factor in the assessed *A. carterae* cultures prior to the nitrogen supplementation.

### *2.2. AMs Accumulation over Different Growth Phases—Comparison of the WT and Mutagenized Strains*

In our study, AM quantities were measured as a function of (i) algal culture growth phase and (ii) strain, while Figure 2 provides a clear visual comparison of the effects of these two factors on AM content.

In the following results and discussion sections, the effects of the growth phase and strain on the cellular AM quota are first examined, as cellular quotas provide biological and mechanistic insight into AM production. Subsequently, the same factors are evaluated for their impact on volumetric AM concentrations, as volumetric concentrations are directly relevant to the biotechnological performance of the AM production process.

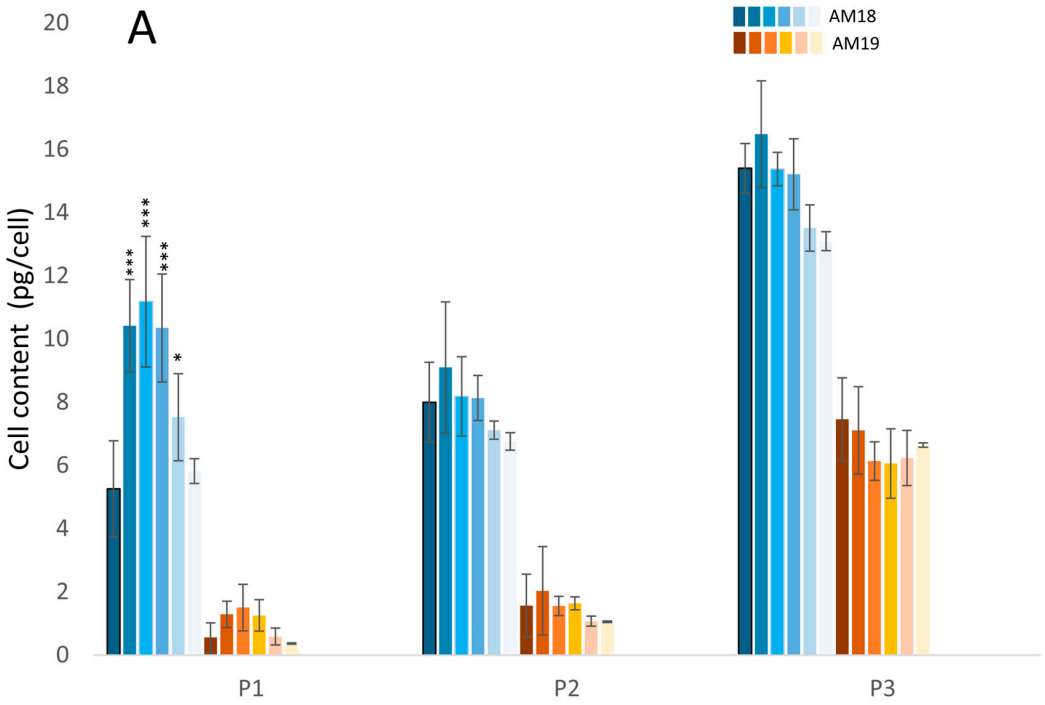


**Figure 2.** *Cont.*

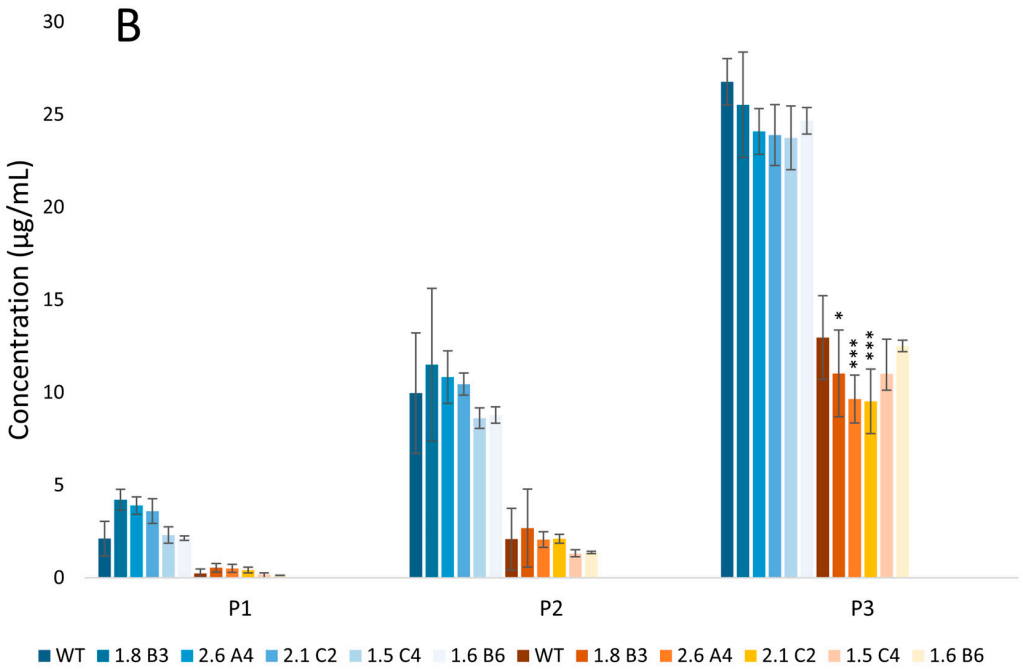


**Figure 2.** (**A**) Amphidinols 18 and 19 cell content and (**B**) volumetric concentrations in wild-type and mutagenized strains at different culture phase. P1, P2 and P3 correspond to the time points positioned in exponential growth, linear growth, and at the first day of the stationary phase, respectively. AM22 quantities were detected at trace levels and are therefore not presented in Figure 2, while the measured values for AM22 are provided in Appendix A Table A2. Asterisks above the error bars show the statistical significance level of the difference in AM concentrations between the WT and mutagenized strains at each sampling point (P1, P2 or P3): (*) $p < 0.05$, and (***) $p < 0.001$. No symbol indicates a non-significant difference. No asterisk is indicated if there is no statistically significant difference between the WT and mutagenized strains at a given time point.

#### 2.2.1. Effect of the Culture Growth Phases on AM Cell Content

Both AM18 and AM19 showed a clear overall increase in cell content from the exponential to the stationary phase. For AM18, this pattern included a slight initial drop from P1 (exponential) to P2 (linear) before rising markedly at P3 (stationary phase) (Figure 2A). This initial AM18 decrease is likely linked to the inoculum, which originated from the transition between the linear and stationary phases and therefore already contained elevated AM18 levels. In contrast, AM19 did not exhibit this initial decline. Instead, its cell content increased steadily from P1 through P3.

Statistical analysis confirmed a significant effect of the growth phase on AM18 and AM19 cellular quotas (two-way ANOVA; $p \leq 0.001$). Post hoc comparisons that used the P1 point as a reference showed that AM18 was lower at P2 and higher at P3 ($p < 0.001$) compared to P1, while AM19 increased significantly from P1 to P2 ($p = 0.028$) and from P1 to P3 ($p < 0.01$).

To expand on these findings, changes in cellular AM content were subsequently quantified as accumulation rates across the P1–P2 and P2–P3 growth intervals to identify the point of the peak AM increase.

The highest per-cell accumulation of AM18 and AM19 occurred between the linear and early stationary growth phases (P2–P3) across all strains. While detailed cell concentration data are provided in Table A2, the maximum per-cell accumulation rates during the P2–P3 interval reached 3.60 ± 0.76 µg/cell/day for AM18 and 2.29 ± 0.24 µg/cell/day for AM19, both observed in strain 2.6 A4.

To the best of our knowledge, no studies have directly quantified changes in AM cell content (or volumetric concentrations) across the different growth phases of *A. carterae*.

Gain and collaborators reported that the inhibitory effect of *A. carterae* on *Thalassiosira pseudonana* PSII increased markedly from the exponential to the stationary phase [31]. They further suggested that rising AM cell concentrations were responsible for the observed increase in inhibition, which aligns with the results obtained in our study. However, the study of Gain and collaborators did not directly measure AM concentrations at the different growth stages of *A. carterae* culture, but rather estimated it as the function of the *T. pseudonana* PSII inhibition.

Our previous study on the same *A. carterae* WT strain examined AM accumulation over a ten-day culture period, but focused exclusively on the stationary phase without evaluating the earlier growth phases [29]. That investigation was conducted under culture conditions comparable to those applied in the present study, including a similar temperature, continuous illumination at a similar irradiance, tubular photobioreactors, and nitrogen-limited growth. Moreover, both the previous and current studies sampled the first day of the stationary phase (P3) and reported similar total AM contents (22.9 $\pm$ 2.0 pg/cell in the present work and 26.9 $\pm$ 6.2 pg/cell previously), demonstrating the strong reproducibility of AM production by *A. carterae* under the applied methodology and conditions.

In our previous study, the highest daily AM18 per-cell content increase during the stationary phase was observed during the first four days of this phase, reaching 1.65 ($\pm$0.70) pg/cell/day [29]. When combining these results with those in the present study, it still can be concluded that the fastest increase in the AM18 cell content in the WT strain occurs between the linear phase (P2) and the first day of the stationary phase (P3). In contrast to AM18, the increase in the AM19 cell content remained relatively constant from P2 to P3, at 1.96 ($\pm$0.89) pg/cell/day, and, during the first four days of the stationary phase, at 1.94 ($\pm$0.50) pg/cell/day [21]. Importantly, both periods, from P2 to P3 and during the first four days of the stationary phase, showed higher AM19 per-cell accumulation rates compared to the other growth intervals studied in our current and our previous study (e.g., growth period between P1 and P2 or period of late stationary phase).

To the best of our knowledge, none of the previous studies tackled the question of AMs dynamics in *Amphidinium* sp. and discussed that information within physiological or ecological contexts. In contrast, polyketide toxins structurally similar to AMs, called karlotoxins, are more frequently elaborated on in the literature due to their cell content change across the different cell growth phases [32,33]. Our observation that AM cell content increases from the linear to stationary growth phases mirrors the patterns reported for karlotoxins in the dinoflagellate species *Karlodinium veneficum* [33].

The observed growth-phase-dependent accumulation also provides a basis for interpreting the ecological function of AMs. Since AMs are known to act as allelochemicals [31,34], the peak of their production between the linear and stationary growth phases may reflect a strategy to load cells with AMs before division slows, thereby maximizing both their competitive advantage over other microalgae as nutrients decline and chemical defense against grazers at this critical ecological transition [35,36]. These findings support the idea that AMs play both competitive and defensive roles during the transition to the stationary phase, as is the case for karlotoxins [33].

Future studies assessing AM accumulation under varying environmental and physiological conditions will be essential to understand fully how AM production is regulated and deployed by *A. carterae*. Moreover, the results presented here may provide a useful baseline for such ecological investigations by offering the first detailed characterization of AM dynamics across distinct growth phases.

2.2.2. Differences Between the Strains' AM Cell Content

A two-way ANOVA revealed a highly significant effect of strain on the AM18 cell content, with a confidence level of 99.9% ($p \leq 0.001$). In contrast, no statistically significant differences were observed among strains regarding the AM19 cell content. The WT strain was used as the reference group in the analysis. Post hoc comparisons indicated that, among strains, the biggest difference in the AM18 content occurred at a high growth rate (P1 time point), as highlighted by the asterisks in Figure 2A.

Among the mutagenized strains, 2.6 A4, 1.8 B3, and 2.1 C2 exhibited the highest AM18 cell content at P1, with mean values of 11.18 (±2.06), 10.41 (±1.46), and 10.35 (±1.73) pg/cell, respectively. These values were more than twice those of the WT strain, which showed a mean AM18 cell content of 5.26 (±1.54) pg/cell at P1. Such results strongly indicate that mutagenesis affected AM18 cell content in these three strains, a conclusion also supported by the large number of biological replicates used for each strain. For strains 2.6 A4, 1.8 B3, and 2.1 C2, the AM18 cell quotas mentioned were based on six replicates across two temporally separated experiments (triplicates in each experiment). Moreover, for the WT strain, nine replicates distributed across three experiments (triplicates in each experiment) were analyzed (see methodological Section 3.1.4 on how culture replicates of different strains were organized temporally).

At sampling point P2 and P3, no significant differences in the AM18 and AM19 cell quotas were found (Figure 2A), unlike at point P1. From an industrial point of view, these points (P2 and P3) may be more interesting than P1 for harvest due to the higher cell concentration. Therefore, future experiments should be conducted to confirm if the observed cell quota differences in P1 can be translated into the improved industrial production of AM18 by strains 2.6 A4, 1.8 B3, and 2.1 C2 compared to the WT strain. As a perspective, the optimization of the growth conditions at a pilot scale could be conducted for the three selected strains and subsequently compared with the WT for AM18 production using a techno-economic analysis. Finally, while the extended cultivation period of all mutagenized strains preceding this study (≈2 years) supports the stability of the phenotypic differences observed between the strains, further monitoring over longer time scales will be valuable to confirm the long-term persistence of these differences.

In the context of previously published data, the AM18 cell quotas measured in this study are higher than values reported in the literature for *Amphidinium* spp. For example, Wellkamp and collaborators reported a total amphidinol cell content between ~0.5 and 3.7 pg/cell across several *Amphidinium* strains, while some of the *A. carterae* strains assessed in their study produced no AMs. Durán-Riveroll and collaborators reported a maximum amphidinol cell content of ~1.7 pg/cell [22] among several strains of *A. carterae* samples initially isolated from the cost of Mexico. In contrast, the present work identifies mutagenized strains with AM18 quotas reaching 13.10 (±0.30)–16.50 (±0.1.69) pg/cell at P3, and a WT strain reaching 15.4 (±0.78) pg/cell at the P3. These comparisons indicate that the strains characterized here, particularly WT and 1.8 B3, exhibit exceptionally high AM18 production. The observed differences between our values and those reported in the literature likely reflect strain-specific biosynthetic capacities and distinct cultivation regimes. Notably, in the two mentioned studies reporting AM cell contents, the *A. carterae* material originated either from Erlenmeyer flasks cultures (Durán-Riveroll and collaborators) or from laboratory cultures grown in bubble column photobioreactors (as in the study by Wellkamp), without controlled pH regulation or $CO_2$ supply in the case of both studies. In contrast, the present study relied on photobioreactor systems that provide pH regulation, active $CO_2$ injection and optimized light delivery. As AMs contain long carbon chains, their biosynthesis depends on sufficient inorganic carbon availability. Cultures grown with an actively supplied carbon source, such as the $CO_2$ injection used in our study, are therefore

likely to accumulate higher levels of AM precursors and ultimately achieve higher AM cell contents compared to cultures without $CO_2$ supplementation. Moreover, while the AM values at P3 in our study were obtained from cultures that entered nitrogen-limiting conditions, the *Amphidinium* cultures analyzed by Durán-Riveroll and Wellkamp may not have been nitrogen-limited (even the corresponding data is not published). If that is the case for the studies by Durán-Riveroll and Wellkamp, the use of nitrogen-limited conditions in our work may represent an additional explanation for the higher AM cell quotas observed in our study, since nitrogen limitation is known to stimulate the production of carbon-rich secondary metabolites such as AM [28].

#### 2.2.3. Effect of the Culture Growth Phases—AM Volumetric Concentration

Both AM18 and AM19 showed a consistent overall increase in volumetric concentration from the exponential to the stationary phase, following a similar pattern observed for their cell content. For AM18, the volumetric concentration rose steadily from P1 through to P3 without displaying the slight initial drop seen at the per-cell level. This difference is explained by the rapid increase in cell density between P1 and P2, which compensated for the temporary reduction in AM18 cell content and resulted in a net volumetric AM18 concentration increase (Figure 2B). AM19 followed a similar upward trajectory to AM18, with higher concentrations at P2 and P3 compared with P1.

Statistical analysis confirmed a significant effect of the growth phase on volumetric AM18 and AM19 concentrations (two-way ANOVA; $p \leq 0.001$). Post hoc comparisons with reference at P1 showed that AM18 concentrations were lower at P1 than at P2 and P3 ($p < 0.001$), while AM19 concentrations increased significantly from P1 to P2 ($p = 0.01$) and from P1 to P3 ($p < 0.001$).

To expand on these findings, the next step was to quantify the changes in AM volumetric concentrations during the two culture intervals (P1 to P2 and P2 to P3) and identify where the greatest AM productivity occurs. Across all strains, volumetric AM concentrations increased more in the P2 to P3 period than in the P1 to P2 period, similarly to what was observed for the AM18 cell content. The average increase in AM18 volumetric concentrations between P2 and P3 (also referred to as AM18 productivity) ranged across strains, from 5.29 ± 0.39 for strain 1.6 B6 to 6.63 ± 0.55 µg/mL/day for strain 2.6 A4. For AM19, the productivity in the same period ranged across strains, from 3.18 ± 0.39 for strain 2.1 C2 to 3.79 ± 0.52 µg/mL/day for strain 2.6 A4. When extending the comparison to the stationary phase, the AM18 and AM19 productivities of the WT strain between P2 and P3 were higher than the productivities previously reported for the same strain over the stationary phase in our earlier study [29].

Altogether, this information suggests that the fastest increase in AM18 and AM19 volumetric concentrations occurs between the linear growth and early stationary phase in conditions that this study used, similarly to what was demonstrated for AM cell contents. However, in industrial production set ups, where the light irradiances used are commonly higher (>200 µmol photons$m^{-2}$·$s^{-1}$), the peak of AM productivity in the tested strains may be shifted. For instance, it has been shown for the WT strain that as irradiance increases from 30, over 60 and 120, to 200 µmol photons$m^{-2}$·$s^{-1}$, the peak of AM productivity tends to shift from the late to the early stationary phase [29]. This implies that the higher the irradiance is, the earlier the peak of the AM productivity may occur. Therefore, when using irradiances higher than those in this study (e.g., >200 µmol photons$m^{-2}$·$s^{-1}$ like in the industry), the observed peak in AM productivity between P2 to P3 may be shifted closer to P2 (the linear growth phase). Consequently, for the industrial production of *A. carterae* in continuous mode with ongoing (non-stop) harvesting, maintaining the culture around the linear growth phase may result in the highest AM productivity. Moreover, in batch or

semi-batch industrial production, AM productivity could be maximized by increasing the proportion of time that the culture remains in the linear growth phase and by harvesting during this phase, while minimizing the culture lag phase time as much as possible.

#### 2.2.4. Differences Between the Strains—AM Volumetric Concentration

A two-way ANOVA showed no effect of the strain on AM18 or AM19 volumetric concentration ($p = 0.102$ and $p = 0.139$ for AM18 and AM19 respectively). Unlike the cell content for AM18 and AM19, the culture volumetric concentration of AMs of the mutagenized strains was not different from that of the WT strain in any of the sampling points (P1, P2 and P3). Additionally, no significant differences were found in AM volumetric productivity within the P2-to-P3 period among the strains tested (Figure 2B). These results suggest that, under the tested culture conditions, the mutagenized strains have not demonstrated considerable improvement over the WT from an industrial perspective, given that increasing AM volumetric productivity is the primary objective for industrial AMs production. Nevertheless, changing culture conditions may allow mutagenized strains to express superior AM productivity per culture volume compared to WT strains, as they have shown in the case of per-cell content at the P1 time point. Therefore, the further optimization of culture conditions for each of the mutagenized strains may be an important step to prove if targeted mutagenized strains can outperform WT Ams in terms of productivity under comparable production costs. Moreover, even if AM volumetric productivity in mutagenized strains was not proven as better than in WT strains after condition optimization steps in the future, these mutagenized strains may provide a useful model for studying genetic differences relative to the WT and linking these differences to observed variations in AM production.

### *2.3. AM Ratios Change over Different Growth Phases—Comparison of the WT Strain and the Mutagenized Strains*

In this study, the focus was placed on analyzing the intracellular ratio of antimicrobially active AM18 to its sulfated inactive counterpart AM19 in *A. carterae* ICC0001. The ratio was studied as a function of the culture growth phase and strain type, and the results are visualized in Figure 3.

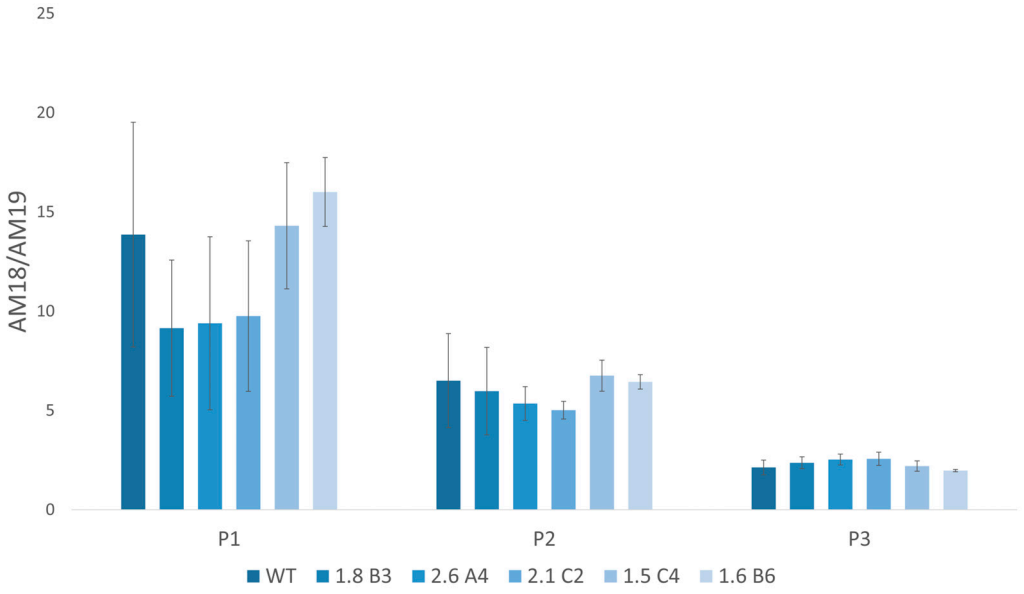


**Figure 3.** Ratio between AM18 and AM19 in wild-type and mutagenized strains over time. P1 corresponds to the exponential growth phase, P2 to the linear growth phase, and P3 to the first day of the stationary phase. Error bars represent the standard deviation of the AM18/AM19 ratio among biological replicates for each strain.

The high standard deviation in the AM18/19 ratio among the replicates for the P1 point observed in Figure 3 arises from intrinsic biological heterogeneity at early growth stages, where amphidinol production and relative compound proportions can fluctuate more strongly between replicates. Moreover, this variability is unlikely to originate from analytical or quantification uncertainty, as the AM18 and AM19 concentrations measured in P1 ranged from approximately 2.1 to 4.2 µg/mL and from 0.13 to 0.57 µg/mL, respectively, which are ranges well above the limit of quantification of the analytical method (LOQ = 0.06 µg/mL for AM18).

As shown in Figure 3, the highest AM18/19 ratio was observed at the P1 point and ranged from 9.39 (±4.36) for 2.6 A4 to 16 (±1.70) for 1.6 B6 (see all numeric values in Appendix A Table A2). In contrast, the lowest AM18/19 ratio was demonstrated for P3, ranging from 1.97 (±0.05) for 1.6 B6 to 2.56 (±0.32) in 2.1 C2 (Appendix A Table A2).

The two-way ANOVA test showed that the progression of culture growth from the exponential to stationary phase significantly lowered the AM18/19 ratio with a confidence level of 99.9% ($p < 0.001$). A post hoc test revealed that the AM18/AM19 ratio at P1 was different from both the P2 and P3 ratios with the confidence level of 99.9% ($p < 0.001$).

The same decreasing trend for AM18/19 with culture age was also shown in our previous study that investigated this ratio over 10 days within the stationary phase for the same WT strain and under the same culture conditions [29]. In the context of AMs at an industrial scale based on *A. carterae*, increasing the ratio between the active and inactive forms of AMs can be valuable for several reasons. One consideration is that, although detailed studies are still limited, it can be assumed that inactive sulfated AM forms share some significant metabolic pathways with their active non-sulfated counterparts, which could reduce the efficiency of active AM production. For example, the biologically inactive AM19 is the sulfated form of AM18 [21], whereas AM18 shows notable antifungal activity [21]. Consequently, the sulfation of AM18 into AM19, and/or the diversion of AM18 precursors toward AM19 biosynthesis, may decrease the fraction of cellular metabolic resources ultimately allocated to the production of active AM forms (AM18). Furthermore, when the goal is to isolate only the active compound such as AM18, the presence of structurally similar inactive forms may act as impurities, increasing the complexity and cost of the purification process.

Taking together, the ideal scenario for harvesting *A. carterae* culture for AM18 production will target a culture with an AM18/19 ratio as high as possible. Therefore, if the highest AM18 productivity occurs between the linear and stationary growth phase as concluded in Section 2.2.3, choosing the harvest closer to the linear phase may result in a higher AM18/19 ratio. This will consequently result in the easier separation of AM18 in case it needs to be purified from the AM mix, and in more efficient use of the cell metabolic resources towards the production of targeted AM18 (instead of its sulfated form, AM19).

Finally, the two-way ANOVA test showed no strain effect on the AM18/19 ratio ($p = 0.081$). Therefore, the strain improvement efforts through the random mutagenesis process have not affected the AM18/19 ratios, thus leaving no mutagenized strains of interest for industry in the context of the improved balance of AM18/AM19.

## 3. Materials and Methods

### *3.1. Algae Cultivation*

To facilitate an overview of the experimental design related to algae cultivation, the following lines briefly summarize it, while the subsequent sections provide detailed descriptions of each experimental step. Algal cultivation was carried out in successive stages. WT and mutagenized *A. carterae* strains were first maintained in Erlenmeyer flasks and were subsequently used to inoculate photobioreactor (PBR) cultures. Two successive

PBR batch cultures were performed: the first, inoculated directly from Erlenmeyer flask cultures, served as an acclimatization step to adapt *A. carterae* to PBR and associated environmental conditions. Cultures from this acclimatization batch were then used as inoculum for the subsequent final batch PBR culture, which was used for AMs analysis and culture growth analysis, as it will be detailed below.

#### 3.1.1. *A. carterae* Strains

The WT strain *Amphidinium carterae* ICC0001 was sourced from the internal microalgal collection maintained by Immunrise Biocontrol France (IBF, Cestas, France). The five mutagenized strains were obtained from the WT strain using the UV mutagenesis as described by Bougaran and collaborators [37], though with one simple difference. Unlike Bougaran and collaborators, this study targeted *A. carterae* cultures with 30% survival rates after UV treatment to achieve the strongest mutagenic effect, as recommended by Rumin and collaborators in a more recent study on microalgal mutagenesis [38]. The five mutagenized strains were selected from the mutagenized strain pool based on their higher antimicrobial activity compared to the WT strain against the yeast *Brettanomyces bruxellensis*, using an antifungal microwell plate test well described elsewhere [39]. These strains were named using randomly generated combinations of numbers and letters (e.g., 1.8 B3).

Importantly, random mutagenesis of the WT *Amphidinium carterae* strain was performed approximately two years prior to the phenotypic evaluations described in this study. During this period, the mutagenized strains were maintained by regular subculturing at monthly intervals.

For experimental preparation of the WT and mutagenized strains, just before the present study, cultivation was carried out in 250 mL Erlenmeyer flasks (Duran Group, Mainz, Germany) using L1 medium [40] at a constant temperature of 20 °C, under a constant light irradiance of 60 µmol photons$m^{-2}{\cdot}s^{-1}$. For Erlenmeyer flask cultivation, the illumination was provided laterally, and the irradiance was measured at the mid-height of the culture volume on the side of the flask facing the light source, using a quantum sensor connected to a LI-250 light meter (LI-COR Biosciences, Lincoln, NE, USA). The L1 medium was prepared using seawater collected near Saint Malo city in France, which was filtered through a 0.22 µm membrane (Millipore, Billerica, MA, USA) and stored in the dark for a minimum of one month. A single, uniform batch of this seawater was used to prepare all the algae culture media used in this study.

#### 3.1.2. PBR Culture Inoculums

Exponential-phase *A. carterae* cultures ($2.5 \pm 0.6 \times 10^5$ cells/mL), including the WT and the five mutagenized strains, grown under the conditions described in Section 3.1.1, were used as the inoculum for photobioreactor (PBR) cultures.

#### 3.1.3. PBR Cultivation and Sampling

To ensure the adaptation of the strains to the final photobioreactor (PBR) conditions, an initial batch culture (referred to as the "acclimatization batch") was performed. Acclimating *A. carterae* prior to experimental cultivation is considered good practice in a number of other studies [29,41]. For acclimatization, inoculums were added to a patented multiple PBR device [42] (Figure 4), with each reactor housing a single strain. This PBR device consists of an array of vertically oriented tubular reactors designed to ensure maximally homogeneous culture conditions across PBRs. The system allows for the regulation of pH (via $CO_2$ injection), irradiance, and aeration flow, while a device's horizontal LED illumination equipped with a diffuser ensures homogeneous irradiance across all reactors. Each PBR contained 300 mL of algae culture in L1 medium with an initial cell concentration of 9.7 ($\pm$0.3) $\times 10^4$ cells/mL, made by diluting the defined inoculum culture volume with

fresh L1 medium. Light irradiance (100 µmol photons·$m^{-2}$·$s^{-1}$), temperature (20 ± 1 °C), ambient air bubbling (0.04 L/min) and pH (8.0), regulated by pure $CO_2$ injection, were controlled across reactors, to keep culture conditions identical among the strains. To avoid significant evaporation in algal cultures during the experiments, the air supplied to the photobioreactors for bubbling was passed through a water saturation system prior to entering the PBRs, while the cultivation temperature was maintained at a moderate level (20 ± 1 °C). For photobioreactor cultures, illumination was provided laterally, and irradiance was measured at the mid-height of the tubular reactor, at a position midway between the reactor surface closest to and farthest from the light source, using a quantum sensor connected to a LI-250 light meter (LI-COR Biosciences, Lincoln, NE, USA).



**Figure 4.** The phenotyping bench device consists of multiple parallel tubular glass photobioreactors (PBRs) equipped with aeration, illumination and pH controls, and pH regulation system using $CO_2$ injection.

The described cultivation parameters were selected to match those used in our previous study [29], thereby ensuring the direct comparability of the amphidinol production dynamics across the growth phases.

All culture manipulations (including PBR inoculation) were performed under sterile conditions in a laminar flow hood, using sterile material (PBRs, tubing/connectors and sampling vessels) to minimize contamination. Cultures from PBRs were monitored daily by light microscopy, and no signs of contamination by other microalgal species were observed during the experimental period.

After 7 days of growth in the mentioned conditions, once all strains had reached the intermediate stage between the linear growth and plateau phases, cultures from the acclimatization batch were harvested and used as inoculum for the subsequent photobioreactor (PBR) cultivation conducted under identical culture conditions, hereafter referred to as the "final batch culture". Pushing *A. carterae* over 7 days was intentionally selected to allow cultures to sequentially pass through the exponential and linear phases, and come close to the stationary growth phase under the target photobioreactor conditions. This way, the cells could physiologically adapt to the applied PBR conditions at each growth phase

prior to the final batch, which was designed to push the cultures to pass through the same growth phases for quantitative analysis.

Each strain from the acclimatization batch was used to inoculate PBRs in the "final batch" in triplicate (three PBR reactors with same strain culture). For each reactor, the inoculum (defined volumes of acclimatized cultures) was diluted in fresh L1 medium to a concentration of 1.75 ($\pm$0.3) $\times$ $10^5$ cells/mL. The total culture volume was 300 mL per reactor. This "final batch culture" was used for all AM analyses conducted in this study.

The "final batch culture" was run for 8 days. Each reactor was harvested once a day for cell counting and AM analysis (by sampling 0.1 mL and 2 mL of culture volume for two analyses, respectively).

#### 3.1.4. "Final Batch Culture" Growth Cycles

Because all strains could not be evaluated at the same time in one single experiment, due to the limited number of available photobioreactors, the complete experimental procedure from inoculum preparation through the acclimatization batch and the final batch culture was carried out in two experiments. Moreover, to obtain a larger set of biological replicates that provides a stronger and more trustworthy basis for the statistical analysis, some of these two experiments were repeated. The following lines explain two experiments and the repetition cycles (Cycle 1 and Cycle 2).

**Cycle 1:** This cycle consisted of two independent experiments (see Figure 5).

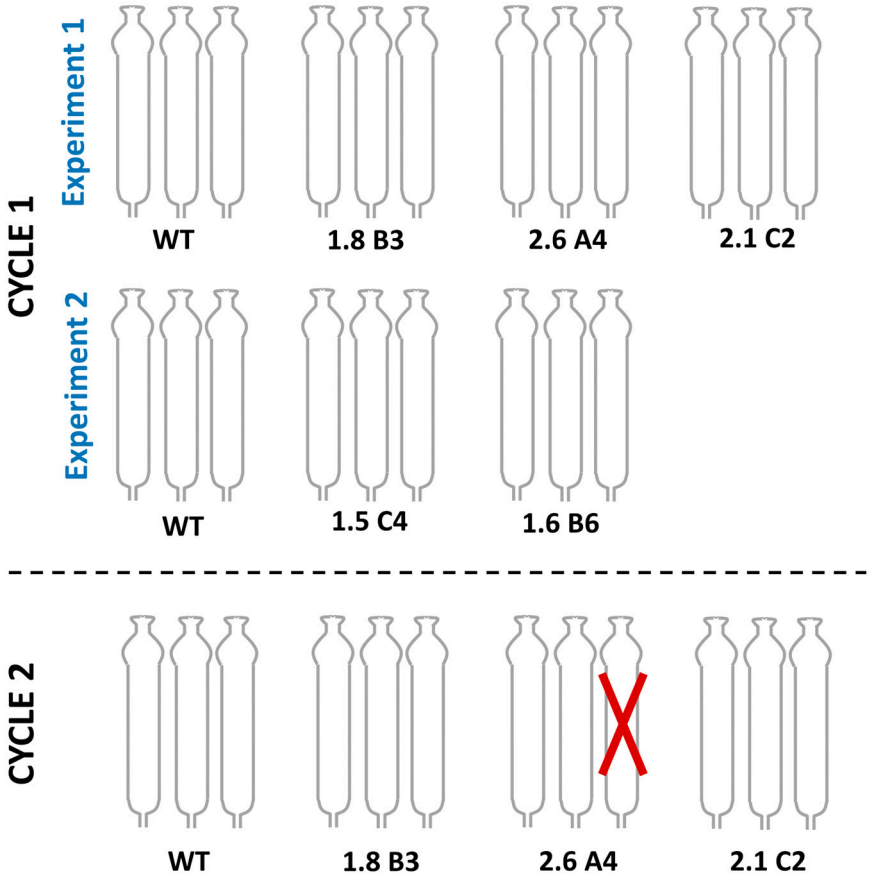


**Figure 5.** Each gray icon represents one photobioreactor (PBR). The red "X" marks the PBR culture of strain 2.6 A4 that was lost during manipulation due to a reactor leak. The spatial arrangement of the PBRs in this schematic does not reflect their actual physical positioning in the multiple PBR device shown in Figure 4, but is intended solely to illustrate the total number of PBRs used in each experimental cycle and for each strain.

In the first experiment, the WT strain was compared with three mutagenized strains (1.8 B3, 2.6 A4 and 2.1 C2). In the second experiment, conducted at a different moment in time but following the same procedure, the WT strain was compared with the two remaining mutagenized strains (1.5 C4 and 1.6 B6). When combined, these two experiments provided data for all five mutagenized strains.

**Cycle 2:** The complete procedure used in Cycle 1 was repeated, but restricted to the WT strain and the three mutagenized strains 1.8 B3, 2.6 A4 and 2.1 C2. A repetition with the other two mutagenized strains (1.5 C4 and 1.6 B6) was not possible because of time and resource limitations.

Accidentally, during Cycle 2, one replicate of strain 2.1 C2 was lost due to a PBR leak. Analyses for this strain were therefore based on five replicates for this strain (three replicates from Cycle 1 and two replicates from Cycle 2).

#### 3.1.5. Proving N Limitation in PBR Cultures

After 8 days of the "final batch culture" of the Cycle 2, 0.075 g/L of $NaNO_3$ (equivalent to the $NaNO_3$ concentration in the standard L1 medium) was added to one replicate of each of the WT, 1.8 B3, and 2.6 A4 strains. The choice of strains and replicates was random. The three cultures chosen were maintained for an additional 20 days under the same conditions, while the other cultures were terminated on day eight. The cell concentration in these three cultures was measured on day 28 (i.e., 20 days after nitrogen addition) using the cell counter (as it will be explained in Section 3.2.1) in order to verify whether growth restarted and new higher cell plateau concentration was reached, thus confirming if the growth was limited by nitrogen.

### *3.2. Sample Treatments and Analyses*

#### 3.2.1. Cell Counting

A volume of 0.1 mL from each culture was diluted in 9.9 mL of 0.2 µm filtered seawater. Cell concentrations were determined using a Multisizer 4 Coulter Counter (Beckman Coulter Inc., Brea, CA, USA) [43].

#### 3.2.2. Growth Kinetics and Specific Growth Rate Calculations

To model the growth kinetics of the algal strains, the modified Gompertz equation was applied, a widely used three-parameter sigmoidal model suitable for describing microbial growth dynamics [25]. The model describes the natural logarithm of cell concentration over time as follows:

$$y = A \cdot exp\{ -exp[ (\mu_m \cdot e/A) \cdot (\lambda - t) + 1 ] \} \quad (1)$$

where

- y is the predicted cell concentration (e.g., ln(N/N0) or cell density depending on the scaling used);
- A represents the asymptotic maximum of the growth curve, corresponding to the upper plateau (final cell concentration level);
- $\mu_{max}$ is the maximum specific growth rate ($day^{-1}$);
- λ denotes the lag time (days), the time before the onset of exponential growth;
- t is the time (days);
- e is Euler's number (≈2.718).

The three biologically meaningful parameters A, $\mu_{max}$ and λ were estimated by nonlinear least squares curve fitting using the lmfit package in Python 3.11 [44], which provides robust minimization and confidence interval estimation.

Firstly, the data fitting procedure was applied to the cell concentration measurements for each culture replicate to obtain replicate level estimates of the three fitting parameters and use them for statistical comparisons among the strains (see Table 1).

Secondly, the fitting was then repeated at the strain level by aggregating the data points from all the culture replicates of a certain strain to generate the visual growth curve representations that will be shown in the results section. All analyses were performed using a custom Python notebook.

#### 3.2.3. Cell Pellets—Sample Preparation and Selection of Samples for AM Analysis

The 2 mL culture samples harvested daily for AM analysis from each culture were centrifuged directly after harvesting at 10,000× *g* for 7 min. The centrifugation was followed by supernatant removal and freezing at −20 °C until the AM analysis.

Out of the biomass samples collected for AM analysis for each "final batch" culture taking one sample during each day of the culture, three samples were selected for chemical analysis, with the main aim of capturing AM levels in distinct growth phases of the culture.

The three samples, each sample corresponding to a different growth phase, were denoted as P1, P2, and P3, with respect to the chronological order of the sampling. This nomenclature will be applied hereafter. P1 corresponds to the day of $\mu_{max}$ to indicate the point when culture grew without limitation (exponential growth phase). P3 is defined as the day when μ dropped below μ = 0.05 ($day^{-1}$), indicating the end of the growth (stationary phase) [29] and full culture growth limitation. Finally, P2 was considered as the middle day between P1 and P3 and reflected the linear growth phase of the culture. When the interval between P1 and P3 consisted of an even number of days (e.g., 4 days), P2 was defined as the later of the two middle days. For example, with a 4-day interval, P2 corresponded to the third day after P1.

#### 3.2.4. Sample Preparation for AM Analysis

Intracellular AMs were extracted by adding LC-MS-grade methanol (methanol ≥99.9%, HiPerSolv CHROMANORM® for HPLC-MS, VWR, Fontenay-sous-Bois, France) to the cell pellet stored in polyethylene tubes containing 0.584–39.2 × $10^5$ cells until a cell concentration of 1.64 (±0.55) × $10^6$ cells/mL was reached. The pellet was resuspended by gentle pipetting and was thoroughly mixed by vortexing at maximum speed for 2 min (VWR International, Radnor, PA, USA).

The tubes were then subjected to sonication using an ultrasonic bath (Transsonic TI H-15, Elma Schmidbauer GmbH, Singen, Germany). Sonication was carried out for 2 min under sweep mode, an ultrasonic frequency of 45 kHz and a power set to 100%. The temperature of the bath was maintained at room temperature.

Cellular debris was removed from methanol by centrifugation at 10,000× *g* for 2 min using a GK15 centrifuge (Fisher Bioblock Sigma, Osterode, Germany). The resulting supernatant was filtered through 0.22 μm polypropylene syringe filters (4 mm, AIT Analytical Instruments, Houilles, France) and collected into 1.5 mL glass vials and stored at −20 °C until LC-MS/MS analysis.

#### 3.2.5. LC-MS/MS Analysis of AMs

The LC-MS/MS analysis of AM18, 19 and 22 was performed as in our previous study [29]. Briefly, the chromatographic separation was performed on a Kinetex C18 column (2.6 μm, 150 × 2.1 mm, Phenomenex, Torrance, CA, USA) using a gradient elution with water and acetonitrile/water phase (95:5, *v*/*v*), both containing ammonium formate and formic acid. Detection by mass spectrometry (API 4000 QTRAP, SCIEX, Framingham, MA, USA) was performed using the parameters presented in Appendix A Table A3.

All the AMs were quantified against an in-house AM-18 standard [29], assuming an equal molar response factor between analogs. Therefore, AM19 and AM22 were expressed as AM18 equivalent.

However, as the AM22 concentrations were commonly around the LQ and LD levels (Appendix A Table A3), the results and discussion will focus on AM18 and AM19.

The LOD and LOQ (assuming a signal-to-noise ratio of three and ten, respectively) for the AM18 standard were 0.02 and 0.06 μg/mL respectively.

Acquisition and data processing were performed using Analyst 1.7.2 (Analyst 1.7.2, SCIEX, Framingham, MA, USA) software.

The quantified AM values were expressed in two units: AM cell content (pg/cell) and AM volumetric concentration (μg/mL). The volumetric concentration corresponds to the total amphidinol measured in the biomass, converted to the equivalent amount per milliliter of algal culture. To improve the readability and avoid repeating the same term throughout the manuscript, alternative terms were also used throughout the text for the two units mentioned. "AM cell content" was occasionally referred to as "AM cell quota", while "AM volumetric concentration" was sometimes referred to as "AM concentration in culture". Finally, the term AM "productivity" was used to indicate the AM volumetric concentration change per day, expressed in unit μg/mL/day.

### 3.3. Data Analysis

The effects of (i) culture age and (ii) strain (WT and the five mutagenized strains) on AM quantities, and AM18/AM19 ratios were assessed using a two-way ANOVA and the Holm–Sidak post hoc test. The statistical significance of the differences in the growth curve fitting parameters A and $\mu_{max}$ among the strains was evaluated using a one-way ANOVA followed by the same post hoc test. All the statistical tests were performed using SigmaPlot 15.0 (Grafiti LLC., New York, NY, USA), which automatically assesses data normality as part of its default workflow prior to applying parametric tests.

## 4. Conclusions

In a world facing a crisis of food contamination and the need for sustainable pesticide alternatives, algal secondary metabolites like amphidinols (AMs) may play a crucial role in the future. This study explored the dynamics of AMs over different culture growth phases in WT strains and five mutagenized *A. carterae* strains, as well as the relevance of this dynamic in future biotechnological applications. The highest AM18 and AM19 productivity occurred during the 3–4 day period between the linear growth (P2) and early stationary phase (P3), with the average values across strains being 5.29 (±0.39) and 6.63 (±0.55) μg/mL/day for AM18 and AM19, respectively. Notably, the ratio between biologically active AM18 and its inactivated sulfated form AM19 decreased with culture age in all strains, with an average decrease of 9.78 (±2.93), from P1 (exponential) to P3 (first day of stationary phase). Altogether these results suggest that harvesting *A. carterae* culture at an earlier point between the linear and early stationary phases provides the best condition for valorizing both the AM18 productivity peak and a favorable ratio of biologically active versus inactive Ams, the mutagenized strains showed that UV-induced random mutagenesis can substantially modify AM biosynthesis, with three mutagenized strains displaying more than a twofold increase in AM18 cell content during the exponential phase compared with the WT strain. Moreover, mutagenesis led to an increase in maximal growth rates up to 20%, as was observed in one of the mutagenized strains. However, these advantages obtained in mutagenized strains did not translate into higher volumetric productivity or improved AM18/19 ratios in the period between the linear and stationary phases when the industrial harvest of culture for AM production was found to be optimal.

Therefore, further culture condition optimization is required for mutagenized strains to determine whether the observed enhancements in cell AM18 content and growth rate can be converted into true productivity gains under industrial conditions. Overall, this study provides the first detailed characterization of the optimal AM harvesting window for their industrial production, and is among the earliest studies published demonstrating the feasibility of random mutagenesis improvement of AM yields in *A. carterae*. Altogether, these findings lay a solid foundation for future strain optimization and the industrial development of AM production.

**Author Contributions:** I.C.: Conceptualization, investigation, formal analysis, writing—original draft, writing—review and editing, data curation, methodology, project administration, and visualization. G.B.: Conceptualization, investigation, and writing—review and editing. B.S.-J.: Conceptualization, and investigation, writing—review and editing. F.H.: Conceptualization, investigation, formal analysis, writing—original draft, writing—review and editing, and data curation. D.R.: Conceptualization and writing—review and editing. C.E.K.: Conceptualization and writing—review and editing. F.M.: Conceptualization. All authors have read and agreed to the published version of the manuscript.

**Funding:** This work was supported by Immunrise Biocontrol France and by the French Ministry of Higher Education, Research and Innovation (MESRI) through the CIFRE program [CIFRE grant N°2022/1537], managed by the National Association for Research and Technology (ANRT).

**Institutional Review Board Statement:** Not applicable.

**Data Availability Statement:** The original contributions presented in this study are included in the article. Further inquiries can be directed to the corresponding author.

**Acknowledgments:** We would like to express our gratitude to Aurélie Charrier, Clarisse Hubert, Elise Evrard and Léna Gouhier for their invaluable technical assistance during the experimental work. Their support and expertise greatly contributed to the successful completion of this study.

**Conflicts of Interest:** The corresponding author and Cyril El Khoury are employed by Immunrise Biocontrol France, which provided part of financial support for this study. The funding body had no involvement in the study design; data collection, analysis, or interpretation; manuscript preparation; or the decision to publish the results. All other authors declare no conflicts of interest.

## Appendix A

**Table A1.** *p*-values for pairwise comparisons of the growth parameters A and $\mu_{max}$ between WT and each mutagenized *A. carterae* strain.

| Comparison | *p*-Value Comparison of A Parameter | *p*-Value Comparison of-$\mu_{max}$ |
|---|---|---|
| WT vs. 1.6 B6 | 0.001 | <0.001 |
| WT vs. 2.1 C2 | 0.002 | <0.001 |
| WT vs. 1.8 B3 | 0.002 | <0.001 |
| WT vs. 1.5 C4 | 0.003 | <0.001 |
| WT vs. 2.6 A4 | 0.006 | 0.158 |

**Table A2.** Concentration of the AMs quantified by MS/MS in three growth phases (P1, P2 and P3) and AM18/AM19 ratio for WT strain and five mutagenized strains (1.8 B3, 2.6 A4, 2.1 C2, 1.5 C4 and 1.6 B6) grown in two experimental cycles (see Section 3.1.4).

| | | | AM18 | AM19 | AM22 | AM18 | AM19 | AM22 | AM18/AM19 |
|---|---|---|---|---|---|---|---|---|---|
| **Cycle** | **Strain** | **Phase** | **Concentration (pg/Cell)** | | | **Concentration (µg/mL)** | | | |
| C1 | **WT** | P1 | 4.32 | 0.22 | <LD | 1.55 | 0.08 | <LD | 19.38 |
| C1 | **WT** | P1 | 5.6 | 0.27 | <LD | 1.9 | 0.09 | <LD | 21.11 |

**Table A2.** *Cont.*

| | | | AM18 | AM19 | AM22 | AM18 | AM19 | AM22 | AM18/AM19 |
|---|---|---|---|---|---|---|---|---|---|
| **Cycle** | **Strain** | **Phase** | **Concentration (pg/Cell)** | | | **Concentration (µg/mL)** | | | |
| C1 | **WT** | P1 | 4.36 | 0.28 | <LD | 1.59 | 0.1 | <LD | 15.9 |
| C1 | **WT** | P1 | 4.33 | 0.27 | <LD | 1.37 | 0.09 | <LD | 15.22 |
| C1 | **WT** | P1 | 4.31 | 0.28 | <LD | 1.49 | 0.1 | <LD | 14.9 |
| C1 | **WT** | P1 | 3.11 | 0.17 | <LD | 1.04 | 0.06 | <LD | 17.33 |
| C2 | **WT** | P1 | 7.32 | 1.25 | <LQ | 3.4 | 0.58 | <LQ | 5.86 |
| C2 | **WT** | P1 | 5.85 | 0.77 | <LD | 2.86 | 0.38 | <LD | 7.53 |
| C2 | **WT** | P1 | 8.09 | 1.48 | <LQ | 3.83 | 0.7 | <LQ | 5.47 |
| C1 | **WT** | P2 | 6.54 | 0.98 | <LQ | 7.31 | 1.09 | <LQ | 6.71 |
| C1 | **WT** | P2 | 7.01 | 0.67 | <LD | 7.39 | 0.71 | <LD | 10.41 |
| C1 | **WT** | P2 | 7.49 | 0.89 | <LQ | 7.31 | 0.87 | <LQ | 8.4 |
| C1 | **WT** | P2 | 7.41 | 0.98 | <LD | 8.18 | 1.08 | <LD | 7.57 |
| C1 | **WT** | P2 | 7.66 | 1.03 | <LD | 8.69 | 1.17 | <LD | 7.43 |
| C1 | **WT** | P2 | 6.77 | 0.9 | <LD | 7.39 | 0.98 | <LD | 7.54 |
| C2 | **WT** | P2 | 9.82 | 2.62 | <LQ | 14.92 | 3.98 | <LQ | 3.75 |
| C2 | **WT** | P2 | 10 | 3.67 | 0.03 | 15.21 | 5.58 | 0.04 | 2.73 |
| C2 | **WT** | P2 | 9.29 | 2.33 | <LQ | 13.31 | 3.34 | <LQ | 3.99 |
| C2 | **WT** | P3 | 15.12 | 7.43 | 0.12 | 25.84 | 12.7 | 0.21 | 2.03 |
| C2 | **WT** | P3 | 14.49 | 4.9 | 0.09 | 25.85 | 8.74 | 0.15 | 2.96 |
| C2 | **WT** | P3 | 14.84 | 5.6 | 0.12 | 25.07 | 9.45 | 0.21 | 2.65 |
| C1 | **WT** | P3 | 14.81 | 7.78 | 0.06 | 26.49 | 13.91 | 0.1 | 1.9 |
| C1 | **WT** | P3 | 14.8 | 7.3 | 0.08 | 26.44 | 13.05 | 0.15 | 2.03 |
| C1 | **WT** | P3 | 15.28 | 7.81 | 0.08 | 26.02 | 13.29 | 0.13 | 1.96 |
| C2 | **WT** | P3 | 16.07 | 8.63 | 0.13 | 27.99 | 15.02 | 0.22 | 1.86 |
| C2 | **WT** | P3 | 16.3 | 8.93 | 0.13 | 28.28 | 15.5 | 0.23 | 1.82 |
| C2 | **WT** | P3 | 16.91 | 8.74 | 0.14 | 28.97 | 14.98 | 0.24 | 1.93 |
| C1 | **1.8 B3** | P1 | 10.95 | 1 | <LD | 4.2 | 0.38 | <LD | 11.05 |
| C1 | **1.8 B3** | P1 | 12.37 | 1.13 | <LQ | 4.87 | 0.45 | <LQ | 10.82 |
| C1 | **1.8 B3** | P1 | 9.07 | 0.61 | <LD | 3.29 | 0.22 | <LD | 14.95 |
| C2 | **1.8 B3** | P1 | 12.11 | 1.77 | <LQ | 3.68 | 0.54 | <LQ | 6.81 |
| C2 | **1.8 B3** | P1 | 8.86 | 1.72 | <LD | 4.58 | 0.89 | <LD | 5.15 |
| C2 | **1.8 B3** | P1 | 9.14 | 1.5 | <LQ | 4.68 | 0.77 | <LQ | 6.08 |
| C1 | **1.8 B3** | P2 | 8.55 | 1.11 | <LQ | 11.68 | 1.52 | <LQ | 7.68 |
| C1 | **1.8 B3** | P2 | 6.88 | 0.82 | <LQ | 5.75 | 0.69 | <LQ | 8.33 |
| C1 | **1.8 B3** | P2 | 7.03 | 0.93 | <LQ | 8.66 | 1.15 | <LQ | 7.53 |
| C2 | **1.8 B3** | P2 | 8.31 | 1.31 | <LD | 9.38 | 1.48 | <LD | 6.34 |
| C2 | **1.8 B3** | P2 | 11.92 | 4.02 | <LQ | 17.34 | 5.84 | <LQ | 2.97 |
| C2 | **1.8 B3** | P2 | 11.89 | 3.97 | 0.03 | 16.2 | 5.41 | 0.04 | 2.99 |
| C1 | **1.8 B3** | P3 | 17.45 | 6.65 | 0.13 | 25.87 | 9.86 | 0.19 | 2.62 |
| C1 | **1.8 B3** | P3 | 15.27 | 6.16 | 0.1 | 23.7 | 9.56 | 0.16 | 2.48 |
| C1 | **1.8 B3** | P3 | 15.83 | 5.6 | 0.1 | 24.26 | 8.59 | 0.16 | 2.82 |
| C2 | **1.8 B3** | P3 | 19.72 | 9.78 | 0.15 | 31.57 | 15.67 | 0.24 | 2.01 |
| C2 | **1.8 B3** | P3 | 14.61 | 6.54 | 0.05 | 23.03 | 10.31 | 0.07 | 2.23 |
| C2 | **1.8 B3** | P3 | 16.02 | 7.89 | 0.08 | 24.75 | 12.2 | 0.12 | 2.03 |
| C1 | **2.6 A4** | P1 | 11.2 | 1.65 | <LD | 4 | 0.59 | <LD | 6.78 |
| C1 | **2.6 A4** | P1 | 7.47 | 0.42 | <LD | 3.03 | 0.17 | <LD | 17.82 |
| C1 | **2.6 A4** | P1 | 11.09 | 1.17 | <LD | 4.28 | 0.45 | <LD | 9.51 |
| C2 | **2.6 A4** | P1 | 13.54 | 2.7 | <LD | 4.31 | 0.86 | <LD | 5.01 |
| C2 | **2.6 A4** | P1 | 12.61 | 1.56 | <LD | 3.88 | 0.48 | <LD | 8.08 |

**Table A2.** *Cont.*

| | | | AM18 | AM19 | AM22 | AM18 | AM19 | AM22 | AM18/AM19 |
|---|---|---|---|---|---|---|---|---|---|
| **Cycle** | **Strain** | **Phase** | **Concentration (pg/Cell)** | | | **Concentration (µg/mL)** | | | |
| C1 | **2.6 A4** | P2 | 8.07 | 1.6 | <LQ | 11.52 | 2.29 | <LQ | 5.03 |
| C1 | **2.6 A4** | P2 | 5.92 | 1.25 | <LQ | 8.06 | 1.7 | <LQ | 4.74 |
| C1 | **2.6 A4** | P2 | 8.31 | 1.27 | <LQ | 11.16 | 1.7 | <LQ | 6.56 |
| C2 | **2.6 A4** | P2 | 8.99 | 2.09 | <LQ | 12.03 | 2.79 | <LQ | 4.31 |
| C2 | **2.6 A4** | P2 | 9.61 | 1.57 | <LQ | 11.41 | 1.86 | <LQ | 6.13 |
| C1 | **2.6 A4** | P3 | 16.32 | 6.01 | 0.14 | 25.45 | 9.37 | 0.22 | 2.72 |
| C1 | **2.6 A4** | P3 | 15.53 | 6.33 | 0.15 | 22.75 | 9.27 | 0.22 | 2.45 |
| C1 | **2.6 A4** | P3 | 14.88 | 5.02 | 0.08 | 22.57 | 7.62 | 0.12 | 2.96 |
| C2 | **2.6 A4** | P3 | 14.9 | 6.74 | 0.11 | 25.32 | 11.46 | 0.19 | 2.21 |
| C2 | **2.6 A4** | P3 | 15.22 | 6.58 | 0.05 | 24.35 | 10.53 | 0.09 | 2.31 |
| C1 | **2.1 C2** | P1 | 7.07 | 0.43 | <LD | 2.95 | 0.18 | <LD | 16.39 |
| C1 | **2.1 C2** | P1 | 9.45 | 0.71 | <LD | 3.89 | 0.29 | <LD | 13.41 |
| C1 | **2.1 C2** | P1 | 12.07 | 1.56 | <LD | 4.94 | 0.64 | <LD | 7.72 |
| C2 | **2.1 C2** | P1 | 10.48 | 1.47 | <LD | 3.07 | 0.43 | <LD | 7.14 |
| C2 | **2.1 C2** | P1 | 11.86 | 1.75 | <LD | 3.5 | 0.52 | <LD | 6.73 |
| C2 | **2.1 C2** | P1 | 11.15 | 1.6 | <LD | 3.26 | 0.47 | <LD | 6.94 |
| C1 | **2.1 C2** | P2 | 7.24 | 1.56 | <LQ | 10.71 | 2.31 | <LQ | 4.64 |
| C1 | **2.1 C2** | P2 | 7.86 | 1.65 | <LQ | 10.84 | 2.28 | <LQ | 4.75 |
| C1 | **2.1 C2** | P2 | 7.3 | 1.24 | <LQ | 9.49 | 1.6 | <LQ | 5.93 |
| C2 | **2.1 C2** | P2 | 9.02 | 1.84 | <LQ | 11.13 | 2.28 | <LQ | 4.88 |
| C2 | **2.1 C2** | P2 | 8.91 | 1.71 | <LQ | 10.76 | 2.06 | <LQ | 5.22 |
| C2 | **2.1 C2** | P2 | 8.46 | 1.82 | <LQ | 9.8 | 2.1 | <LQ | 4.67 |
| C1 | **2.1 C2** | P3 | 13.6 | 5.17 | 0.09 | 21.5 | 8.17 | 0.14 | 2.63 |
| C1 | **2.1 C2** | P3 | 15.29 | 4.98 | 0.1 | 23.77 | 7.74 | 0.15 | 3.07 |
| C1 | **2.1 C2** | P3 | 13.89 | 4.81 | 0.09 | 22.2 | 7.68 | 0.15 | 2.89 |
| C2 | **2.1 C2** | P3 | 16.01 | 6.74 | 0.07 | 24.25 | 10.21 | 0.1 | 2.38 |
| C2 | **2.1 C2** | P3 | 15.77 | 7.23 | 0.07 | 26.11 | 11.98 | 0.12 | 2.18 |
| C2 | **2.1 C2** | P3 | 16.71 | 7.43 | 0.08 | 25.51 | 11.34 | 0.12 | 2.25 |
| C1 | **1.5 C4** | P1 | 6.71 | 0.39 | <LD | 2.03 | 0.12 | <LD | 16.92 |
| C1 | **1.5 C4** | P1 | 6.4 | 0.4 | <LD | 1.96 | 0.12 | <LD | 16.33 |
| C1 | **1.5 C4** | P1 | 9.46 | 0.96 | <LD | 2.93 | 0.3 | <LD | 9.77 |
| C1 | **1.5 C4** | P2 | 7.52 | 1.27 | <LD | 9.39 | 1.58 | <LD | 5.94 |
| C1 | **1.5 C4** | P2 | 6.88 | 0.88 | <LD | 8.15 | 1.04 | <LD | 7.84 |
| C1 | **1.5 C4** | P2 | 6.95 | 1.07 | <LD | 8.3 | 1.27 | <LD | 6.54 |
| C1 | **1.5 C4** | P3 | 14.54 | 7.24 | 0.1 | 25.91 | 12.91 | 0.18 | 2.01 |
| C1 | **1.5 C4** | P3 | 13.12 | 5.11 | 0.05 | 21.7 | 8.45 | 0.08 | 2.57 |
| C1 | **1.5 C4** | P3 | 12.87 | 6.36 | 0.04 | 23.62 | 11.67 | 0.08 | 2.02 |
| C1 | **1.6 B6** | P1 | 6.34 | 0.34 | <LD | 2.28 | 0.12 | <LD | 19 |
| C1 | **1.6 B6** | P1 | 5.7 | 0.39 | <LD | 1.98 | 0.14 | <LD | 14.14 |
| C1 | **1.6 B6** | P1 | 5.41 | 0.36 | <LD | 2.16 | 0.15 | <LD | 14.4 |
| C1 | **1.6 B6** | P2 | 7.12 | 1.04 | <LD | 9.41 | 1.38 | <LD | 6.82 |
| C1 | **1.6 B6** | P2 | 6.69 | 1.03 | <LD | 8.37 | 1.28 | <LD | 6.54 |
| C1 | **1.6 B6** | P2 | 6.46 | 1.08 | <LD | 8.58 | 1.44 | <LD | 5.96 |
| C1 | **1.6 B6** | P3 | 12.92 | 6.74 | 0.07 | 23.65 | 12.33 | 0.13 | 1.92 |
| C1 | **1.6 B6** | P3 | 12.84 | 6.6 | 0.1 | 25.2 | 12.94 | 0.19 | 1.95 |
| C1 | **1.6 B6** | P3 | 13.51 | 6.59 | 0.1 | 25.14 | 12.26 | 0.19 | 2.05 |

**Table A3.** Source parameters and compound detection parameters for the LC-MS/MS analysis of Amphidinol-18 (AM18), Amphidinol-19 (AM19) and Amphidinol-22 (AM22). Transitions in bold are the most intense and are used for quantification.

| **Source Parameters** | | | | |
|---|---|---|---|---|
| **Curtain Gas (psi)** | **Ion Spray Voltage (V)** | **Temperature (°C)** | **Ion Source Gas 1 (psi)** | **Ion Source Gas 2 (psi)** |
| 15 | 2800 | 400 | 35 | 35 |
| Detection parameters | | | | |
| Compound | Precursor Ion Q1 ($m/z$) | Product Ion Q3 ($m/z$) | Declustering Potential (V) | Collision Energy (V) |
| AM18 | **1381.9** | **1105.8** | 370 | 98 |
| | 1381.9 | 687.4 | 370 | 120 |
| | 1381.9 | 1163.8 | 370 | 93 |
| | 1381.9 | 963.6 | 370 | 96 |
| AM19 | **1483.8** | **1363.7** | 370 | 95 |
| | 1483.8 | 1105.7 | 370 | 95 |
| | 1483.8 | 945.8 | 370 | 95 |
| | 1483.8 | 687.6 | 370 | 120 |
| AM22 | 1667.9 | 1329.8 | 350 | 95 |
| | 1667.9 | 991.7 | 350 | 95 |
| | 1667.9 | 1543.8 | 350 | 80 |
| | **1667.9** | **699.5** | 350 | 120 |

## References


1. European Commission Joint Research Centre. *Pesticides Residues in European Agricultural Soils: Results from LUCAS 2018 Soil Module*; Publications Office: Luxembourg, 2023.
2. Ballabio, C.; Panagos, P.; Lugato, E.; Huang, J.-H.; Orgiazzi, A.; Jones, A.; Fernández-Ugalde, O.; Borrelli, P.; Montanarella, L. Copper distribution in European topsoils: An assessment based on LUCAS soil survey. *Sci. Total Environ.* **2018**, *636*, 282–298. [CrossRef]
3. Tamm, L.; Thuerig, B.; Apostolov, S.; Blogg, H.; Borgo, E.; Corneo, P.E.; Fittje, S.; De Palma, M.; Donko, A.; Experton, C.; et al. Use of Copper-Based Fungicides in Organic Agriculture in Twelve European Countries. *Agronomy* **2022**, *12*, 673. [CrossRef]
4. Tadesse Mawcha, K.; Malinga, L.; Muir, D.; Ge, J.; Ndolo, D. Recent Advances in Biopesticide Research and Development with a Focus on Microbials. *F1000Research* **2025**, *13*, 1071. [CrossRef] [PubMed]
5. Schneider, K.; Barreiro-Hurle, J.; Rodriguez-Cerezo, E. Pesticide reduction amidst food and feed security concerns in Europe. *Nat. Food* **2023**, *4*, 746–750. [CrossRef] [PubMed]
6. Asimakis, E.; Shehata, A.A.; Eisenreich, W.; Acheuk, F.; Lasram, S.; Basiouni, S.; Emekci, M.; Ntougias, S.; Taner, G.; May-Simera, H.; et al. Algae and Their Metabolites as Potential Bio-Pesticides. *Microorganisms* **2022**, *10*, 307. [CrossRef]
7. Costa, J.A.V.; Freitas, B.C.B.; Cruz, C.G.; Silveira, J.; Morais, M.G. Potential of microalgae as biopesticides to contribute to sustainable agriculture and environmental development. *J. Environ. Sci. Health Part B* **2019**, *54*, 366–375. [CrossRef]
8. Frankmölle, W.P.; Knübel, G.; Moore, R.E.; Patterson, G.M.L. Antifungal cyclic peptides from the terrestrial blue-green alga Anabaena laxa. II. Structures of laxaphycins A, B, D and E. *J. Antibiot.* **1992**, *45*, 1458–1466. [CrossRef]
9. Méjean, A.; Paci, G.; Gautier, V.; Ploux, O. Biosynthesis of anatoxin-a and analogues (anatoxins) in cyanobacteria. *Toxicon* **2014**, *91*, 15–22. [CrossRef]
10. Berry, J.; Gantar, M.; Perez, M.; Berry, G.; Noriega, F. Cyanobacterial Toxins as Allelochemicals with Potential Applications as Algaecides, Herbicides and Insecticides. *Mar. Drugs* **2008**, *6*, 117–146. [CrossRef]
11. Yann, T.; Odon, T.D.L.C. Use of a Cellular Extract of One or More Microalgae of the *Amphidinium* Genus, for Its Fungicidal and/or Bactericidal Activity on Fungi, Oomycetes and/or Pathogenic Bacteria of Plants and Culture Seeds. U.S. Patent Application 16/308,111 WO/2017/211998, 14 December 2017.
12. Kumar, G.; Shekh, A.; Jakhu, S.; Sharma, Y.; Kapoor, R.; Sharma, T.R. Bioengineering of Microalgae: Recent Advances, Perspectives, and Regulatory Challenges for Industrial Application. *Front. Bioeng. Biotechnol.* **2020**, *8*, 914. [CrossRef]
13. Murray, S. *Diversity and Phylogenetics of Sand-Dwelling Dinoflagellates*; VDM Verlag: Saarbrücken, Germany, 2009.
14. Zhang, Z.; Green, B.R.; Cavalier-Smith, T. Single gene circles in dinoflagellate chloroplast genomes. *Nature* **1999**, *400*, 155–159. [CrossRef] [PubMed]

15. Hackett, J.D.; Anderson, D.M.; Erdner, D.L.; Bhattacharya, D. Dinoflagellates: A remarkable evolutionary experiment. *Am. J. Bot.* **2004**, *91*, 1523–1534. [CrossRef] [PubMed]
16. Steidinger, K.A.; Tangen, K. Dinoflagellates. In *Identifying Marine Diatoms and Dinoflagellates*; Tomas, C.R., Ed.; Academic Press: San Diego, CA, USA, 1995; pp. 387–584.
17. Larsen, J.; Patterson, D.J. Some flagellates (Protista) from tropical marine sediments. *J. Nat. Hist.* **1990**, *24*, 801–937. [CrossRef]
18. Jørgensen, M.F.; Murray, S.; Daugbjerg, N. *Amphidinium* Revisited. I. Redefinition of *Amphidinium* (Dinophyceae) Based on Cladistic and Molecular Phylogenetic Analyses. *J. Phycol.* **2004**, *40*, 351–365. [CrossRef]
19. Russo, N.; Quaini, G.; Ziaco, M.; Castiglia, D.; Ruggiero, A.; D'Amelia, V.; Di Napoli, C.; Esposito, S.; Fontana, A.; Nuzzo, G.; et al. Bioactive Polyketides from *Amphidinium* spp.: An In-Depth Review of Biosynthesis, Applications, and Current Research Trends. *Mar. Drugs* **2025**, *23*, 255. [CrossRef]
20. Morales-Amador, A.; Souto, M.L.; Hertweck, C.; Fernández, J.J.; García-Altares, M. Rapid Screening of Polyol Polyketides from Marine Dinoflagellates. *Anal. Chem.* **2022**, *94*, 14205–14213. [CrossRef]
21. Nuzzo, G.; Cutignano, A.; Sardo, A.; Fontana, A. Antifungal Amphidinol 18 and Its 7-Sulfate Derivative from the Marine Dinoflagellate *Amphidinium carterae*. *J. Nat. Prod.* **2014**, *77*, 1524–1527. [CrossRef]
22. Durán-Riveroll, L.M.; Weber, J.; Krock, B. First Identification of Amphidinols from Mexican Strains and New Analogs. *Toxins* **2023**, *15*, 163. [CrossRef]
23. Iwamoto, M.; Sumino, A.; Shimada, E.; Kinoshita, M.; Matsumori, N.; Oiki, S. Channel Formation and Membrane Deformation via Sterol-Aided Polymorphism of Amphidinol 3. *Sci. Rep.* **2017**, *7*, 10782. [CrossRef]
24. Martínez, K.A.; Lauritano, C.; Druka, D.; Romano, G.; Grohmann, T.; Jaspars, M.; Martín, J.; Díaz, C.; Cautain, B.; De La Cruz, M.; et al. Amphidinol 22, a New Cytotoxic and Antifungal Amphidinol from the Dinoflagellate *Amphidinium carterae*. *Mar. Drugs* **2019**, *17*, 385. [CrossRef]
25. Barone, M.E.; Murphy, E.; Parkes, R.; Fleming, G.T.A.; Campanile, F.; Thomas, O.P.; Touzet, N. Antibacterial Activity and Amphidinol Profiling of the Marine Dinoflagellate *Amphidinium carterae* (Subclade III). *Int. J. Mol. Sci.* **2021**, *22*, 12196. [CrossRef] [PubMed]
26. Wellkamp, M.; García-Camacho, F.; Durán-Riveroll, L.M.; Tebben, J.; Tillmann, U.; Krock, B. LC-MS/MS Method Development for the Discovery and Identification of Amphidinols Produced by *Amphidinium*. *Mar. Drugs* **2020**, *18*, 497. [CrossRef] [PubMed]
27. Cutignano, A.; Nuzzo, G.; Sardo, A.; Fontana, A. The Missing Piece in Biosynthesis of Amphidinols: First Evidence of Glycolate as a Starter Unit in New Polyketides from *Amphidinium carterae*. *Mar. Drugs* **2017**, *15*, 157. [CrossRef] [PubMed]
28. Molina-Miras, A.; Bueso-Sánchez, A.; Cerón-García, M.D.C.; Sánchez-Mirón, A.; Contreras-Gómez, A.; García-Camacho, F. Effect of Nitrogen, Phosphorous, and Light Colimitation on Amphidinol Production and Growth in the Marine Dinoflagellate Microalga *Amphidinium carterae*. *Toxins* **2022**, *14*, 594. [CrossRef] [PubMed]
29. Citakovic, I.; Bougaran, G.; Saint-Jean, B.; Hervé, F.; Réveillon, D.; Bérard, J.-B.; Stachowski-Haberkorn, S.; Thiébeauld, O.; El Khoury, C.; Thomas, Y.; et al. Effect of light and cultivation duration on the dynamics of the intra and extracellular amphidinols in nitrogen deficient *Amphidinium carterae* culture. *Algal Res.* **2025**, *90*, 104195. [CrossRef]
30. Barone, M.E.; Murphy, E.; Fierli, D.; Campanile, F.; Fleming, G.T.A.; Thomas, O.P.; Touzet, N. Bioactivity of Amphidinol-Containing Extracts of *Amphidinium carterae* Grown Under Varying Cultivation Conditions. *Curr. Microbiol.* **2024**, *81*, 353. [CrossRef]
31. Gain, G.; Peltekis, A.; Fontana, A.; Bailleul, B. Measurements of photosynthesis in mixtures reveal allelopathy between a dinoflagellate (*Amphidinium carterae*) and a diatom (*Thalassiosira pseudonana*). *Biochim. Biophys. Acta BBA-Bioenerg.* **2022**, *1863*, 148823. [CrossRef]
32. Broemsen, E.L.J.E.; Wira, J.; Place, A.R.; Parrow, M.W. Influence of mixotrophy on cell cycle phase duration and correlation of karlotoxin synthesis with light and G1 phase in *Karlodinium veneficum*. *Harmful Algae* **2024**, *140*, 102741. [CrossRef]
33. Adolf, J.E.; Bachvaroff, T.R.; Place, A.R. Environmental Modulation of Karlotoxin Levels in Strains of the Cosmopolitan Dinoflagellate, *Karlodinium veneficum* (Dinophyceae). *J. Phycol.* **2009**, *45*, 176–192. [CrossRef]
34. Ji, X.; Han, X.; Yang, B.; Yu, Z. Analysis on allelochemicals in the cell-free Filtrates of *Amphidinium carterae*. *Acta Ecol. Sin.* **2012**, *32*, 1745–1754. [CrossRef]
35. Mejía-Camacho, A.L.; Durán-Riveroll, L.M.; Cembella, A.D. Toxicity Bioassay and Cytotoxic Effects of the Benthic Marine Dinoflagellate *Amphidinium operculatum*. *J. Xenobiotics* **2021**, *11*, 33–45. [CrossRef] [PubMed]
36. Luo, Z.; Wang, N.; Mohamed, H.F.; Liang, Y.; Pei, L.; Huang, S.; Gu, H. *Amphidinium stirisquamtum* sp. nov. (Dinophyceae), a new marine sand-dwelling dinoflagellate with a novel type of body scale. *Algae* **2021**, *36*, 241–261. [CrossRef]
37. Bougaran, G.; Rouxel, C.; Dubois, N.; Kaas, R.; Grouas, S.; Lukomska, E.; Le Coz, J.-R.; Cadoret, J.-P. Enhancement of neutral lipid productivity in the microalga *Isochrysis* affinis *Galbana* (T-Iso) by a mutation-selection procedure. *Biotechnol. Bioeng.* **2012**, *109*, 2737–2745. [CrossRef] [PubMed]
38. Rumin, J.; Carrier, G.; Rouxel, C.; Charrier, A.; Raimbault, V.; Cadoret, J.-P.; Bougaran, G.; Saint-Jean, B. Towards the optimization of genetic polymorphism with EMS-induced mutagenesis in *Phaeodactylum tricornutum*. *Algal Res.* **2023**, *74*, 103148. [CrossRef]

39. Acuña-Fontecilla, A.; Bruna, J.; Ganga, M.A.; Godoy, L. Antimicrobial Activity of Leaf Aqueous Extract of *Schinus polygamus* (Cav.) Cabrera against Pathogenic Bacteria and Spoilage Yeasts. *Plants* **2024**, *13*, 2248. [CrossRef]
40. Guillard, R.R.L.; Hargraves, P.E. Stichochrysis immobilis is a diatom, not a chrysophyte. *Phycologia* **1993**, *32*, 234–236. [CrossRef]
41. Molina-Miras, A.; Morales-Amador, A.; de Vera, C.R.; López-Rosales, L.; Sánchez-Mirón, A.; Souto, M.L.; Fernández, J.J.; Norte, M.; García-Camacho, F.; Molina-Grima, E. A pilot-scale bioprocess to produce amphidinols from the marine microalga *Amphidinium carterae*: Isolation of a novel analogue. *Algal Res.* **2018**, *31*, 87–98. [CrossRef]
42. Bérard, J.-B.; Bougaran, G.; Roig, N.; Carrier, G. Système et Méthode de Culture de Souches de Phytoplancton. French Patent FR3103497, 2021. Available online: https://data.inpi.fr/brevets/FR3103497 (accessed on 9 February 2026).
43. Pageault, L.; Charrier, A.; Saint-Jean, B.; Bougaran, G.; Mairet, F.; Stachowski-Haberkorn, S. Cell Cycle Dynamics in the Microalga *Tisochrysis lutea*: Influence of Light Duration and Drugs. *Cells* **2024**, *13*, 1925. [CrossRef]
44. Newville, M.; Stensitzki, T.; Allen, D.B.; Rawlik, M.; Ingargiola, A.; Nelson, A. *LMFIT: Non-Linear Least-Square Minimization and Curve-Fitting for Python*; Astrophysics Source Code Library: Washington, DC, USA, 2016. [CrossRef]


**Disclaimer/Publisher's Note:** The statements, opinions and data contained in all publications are solely those of the individual author(s) and contributor(s) and not of MDPI and/or the editor(s). MDPI and/or the editor(s) disclaim responsibility for any injury to people or property resulting from any ideas, methods, instructions or products referred to in the content.